HOSTED BY

ELSEVIER

CrossMark

Available online at www.sciencedirect.com

ScienceDirect

Journal of Magnesium and Alloys 3 (2015) 63−69
www.elsevier.com/journals/journal-of-magnesium-and-alloys/2213-9567

Full length article

Dry sliding wear behavior of an extruded Mg−Dy−Zn alloy with long period stacking ordered phase

Guangli Bi*, Yuandong Li, Xiaofeng Huang, Tijun Chen, Ying Ma, Yuan Hao

State Key Laboratory of Advanced Processing and Recycling of Nonferrous Metals, Lanzhou University of Technology, Lanzhou 730050, China

Received 27 October 2014; revised 11 December 2014; accepted 18 December 2014
Available online 31 January 2015

Abstract

The dry sliding wear behavior of extruded Mg-2Dy-0.5Zn alloy (at.%) was investigated using a pin-on-disk configuration. The friction coefficient and wear rate were measured within a load range 20−760 N at a sliding velocity of 0.785 m/s. Microstructure and wear surface of alloy were examined using scanning electron microscopy. The mechanical properties of alloy were tested at room and elevated temperatures. Five wear mechanisms, namely abrasion, oxidation, delamination, thermal softening and melting dominated the whole wear behavior with increasing applied load. The extruded Mg-2Dy-0.5Zn alloy exhibited the better wear resistance as compared with as-cast $Mg_{97}Zn_1Y_2$ alloy under the given conditions through contact surface temperature analysis. The improved wear resistance was mainly related to fine grain size, good thermal stability of long period stacking order (LPSO) phase and excellent higher-temperature mechanical properties.

Keywords: Mg−Dy−Zn alloy; Coefficient of friction; Wear rate; Wear mechanism

1. Introduction

Magnesium alloys have become promising materials as structural components in the aerospace and automobile industries because of their low density, high specific strength and damping capacity. However, Mg alloys usually exhibit poor wear resistance, which strongly limits their further applications at some extent. Thus, it is necessary to develop friction and wear properties of Mg alloys for the applications of many other parts such as the components around the engine parts [1].

The friction and wear properties of Mg alloys are mainly affected by the surface microstructure of Mg alloys. The previous investigations have demonstrated that micro alloying [2], cryogenic treatment [3,4], hot working [5,6] and introduction of some dispersoids [7] could effectively improve the surface microstructure to enhance friction and wear properties of Mg alloys. For example, some dispersoids, such as fine ceramics and oxide particles, are usually introduced into microstructures intentionally to induce grain refinement and restrict grain growth. Recently, Somekawa et al. [1] investigated the friction and wear properties of Mg-Zn−Y alloy with dispersion of quasi-crystalline phase. The corresponding experimental results indicated that the homogenous dispersive distribution of the quasi-crystalline phase in the coarse-grained matrix significantly enhances wear properties of the alloy. Similar to quasi-crystalline phase, the long period stacking order (LPSO) structure is an ideal strengthening phase for Mg alloys, whose unit cell contains different closed-packed planes. Various types of LPSO structures, including 6H, 10H, 14H, 18R and 24R types, have been observed in as-cast and heat-treated Mg-RE-Zn alloys (where RE represents Y, Gd, Er and Dy) [8−17]. Among them, 18R and 14H types are commonly observed and the 18R type could transform into

* Corresponding author. Tel./fax: +86 931 2973564.
E-mail address: glbi@163.com (G. Bi).
Peer review under responsibility of National Engineering Research Center for Magnesium Alloys of China, Chongqing University.

http://dx.doi.org/10.1016/j.jma.2014.12.006.

14H type during heat treatment. The LPSO phase has good thermal stability, high hardness value and a coherent interface with Mg matrix. The extruded Mg-RE-Zn alloys containing a large volume fraction of LPSO phases have been confirmed to show superior tensile strengths and available ductility at both room and elevated temperatures [11,17,18]. However, the investigation on friction and wear properties of these alloys was seldom reported. Up to now, An et al. [19] have investigated dry sliding wear behavior of as-cast $Mg_{97}Zn_1Y_2$ alloy. They pointed out that the alloy exhibits better wear resistance than AZ91 alloy due to the superior thermal stability of $Mg_{12}Y_1Zn_1$ phase with LPSO structure. Hu et al. [20] also studied dry sliding behavior of cast Mg-11Y-5Gd-2Zn magnesium alloy. They confirmed that the wear resistance of as-cast + T6 heat-treated alloy is higher than that of as-cast one originating from the precipitation of a large amount of $Mg_{12}Y_1Zn_1$ phases. In our published work, the microstructure, mechanical and corrosion properties of as-cast, extruded and aging heat-treated Mg-2Dy-0.5Zn (at.%) alloy have been investigated, respectively [21]. The extruded Mg-2Dy-0.5Zn alloy exhibits excellent mechanical properties, especially at 300 °C. However, the friction and wear behavior of the alloy has not been investigated until now.

In the present paper, to further understand wear behavior of the alloy, the dry sliding wear and friction properties of extruded Mg-2Dy-0.5Zn alloy were investigated using a pin-on-disc configuration. The as-cast $Mg_{97}Zn_1Y_2$ alloy reported by An et al. [19] was selected as the contrast one. The effect of applied load and contact temperatures on the wear mechanism was also discussed.

2. Experimental procedures

The experimental Mg-2Dy-0.5Zn (at.%) alloy was prepared from pure Mg, pure Zn and Mg-(20wt.%)Dy master alloy in a graphite crucible under an anti-oxidizing flux. The melts were homogenized at 750 °C for 0.5 h and then were poured into a water-cooling mould of a diameter of 85 mm and a length of 350 mm at 720 °C. The ingots were homogenized at 525 °C for 10 h and were machined into the round bars with a diameter of 80 mm. The bars were extruded by an extrusion ratio of 17 at 360 °C and then were aged at 180 °C for 99 h.

The calorimetric response of the alloy was measured using differential scanning calorimetry (DSC) (STA449C). A heating rate of 6 °C/min was employed under argon purge at 35 ml/min. Microstructure, phase structure and composition of alloy were characterized by optical microscope (OM) (Olym-pusGX71), scanning electron microscope (SEM) (JSM-6700F) with energy dispersive X-ray spectroscopy (EDS) (INCA from Oxford). Samples for optical and scanning electron microscope observations were polished and then etched in a solution of 4 ml nitric and 96 ml ethanol. Tensile tests were carried out in an Instron-type tensile testing machine (Instron 1211) at room temperature (RT), 100, 200 and 300 °C, respectively, with a strain rate of $1 \times 10^{-3}s^{-1}$ for all the specimens tested. The tensile specimens with a gauge dimension of 40 mm × 5 mm × 1.8 mm were cut from the heat-treated bars with their length direction parallel to the extrusion direction.

Dry sliding friction and wear tests were carried out with a pin-on-disc type machine at a room temperature of 25 °C. The disc of 70 mm diameter was made of high carbon chromium steel. The bearing surface of the disc was ground to a constant surface roughness. The disc rotation speed was kept at 78.5×10^{-2} ms^{-1}. Specimens of 6 mm diameter × 12 mm length were machined from the heat-treated bars. Specimen surfaces were polished and thoroughly degreased by acetone. Specimens were weighted on an electronic balance with a precision of 0.1 mg before and after wear test. The worn surface of the wear pins was examined with a JSM-6700F scanning electron microscope.

3. Results and discussion

3.1. Microstructure and mechanical properties

Fig. 1 shows the DSC curve of extruded Mg-2Dy-0.5Zn alloy. During continuous heating two endothermic peaks are observed at 539.5 °C and 626.6 °C, respectively. According to the Mg–Dy binary phase diagram [22], the first endothermic peak (539.5 °C) corresponds to dissolution of the eutectic phase and the second one (626.6 °C) corresponds to melting of the matrix, this result is also reported by Peng et al. [23]. Microstructure of alloy is mainly composed of α-Mg matrix, $(Mg, Zn)_xDy$ particle and a large number of 14H-type LPSO phases. It can be seen from Fig. 2(a) and (b) that the morphology of LPSO phase can be classified as two kinds: one is the block-shape, which mainly distributes along the extrusion direction and the other is the fine lamellar-shape in the grain interior as shown in Fig. 2(c). The average grain size of alloy is about 3 μm. Fig. 3 shows the tensile properties of extruded Mg-2Dy-0.5Zn alloy and as-cast $Mg_{97}Zn_1Y_2$ alloy at room and elevated temperatures. With increasing testing temperature, yield strength ($\sigma_{0.2}$), ultimate tensile strength (σ_b) of two alloys significantly decrease, but the elongation to failure (ε) gradually increases. In addition, $\sigma_{0.2}$, σ_b and ε of extruded Mg-2Dy-0.5Zn alloy are higher than that of as-cast $Mg_{97}Zn_1Y_2$ alloy, especially at elevated temperatures [18].

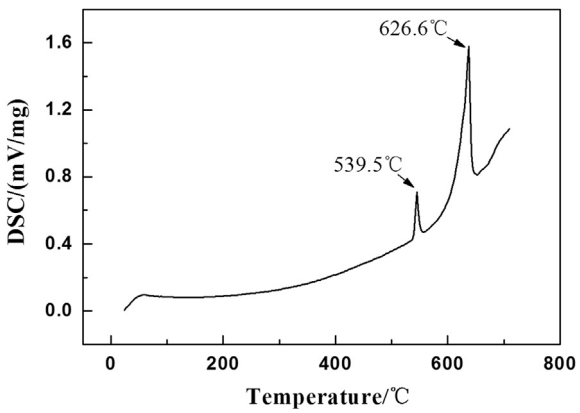

Fig. 1. DSC curve of extruded Mg-2Dy-0.5Zn alloy aged at 180 °C for 99 h.

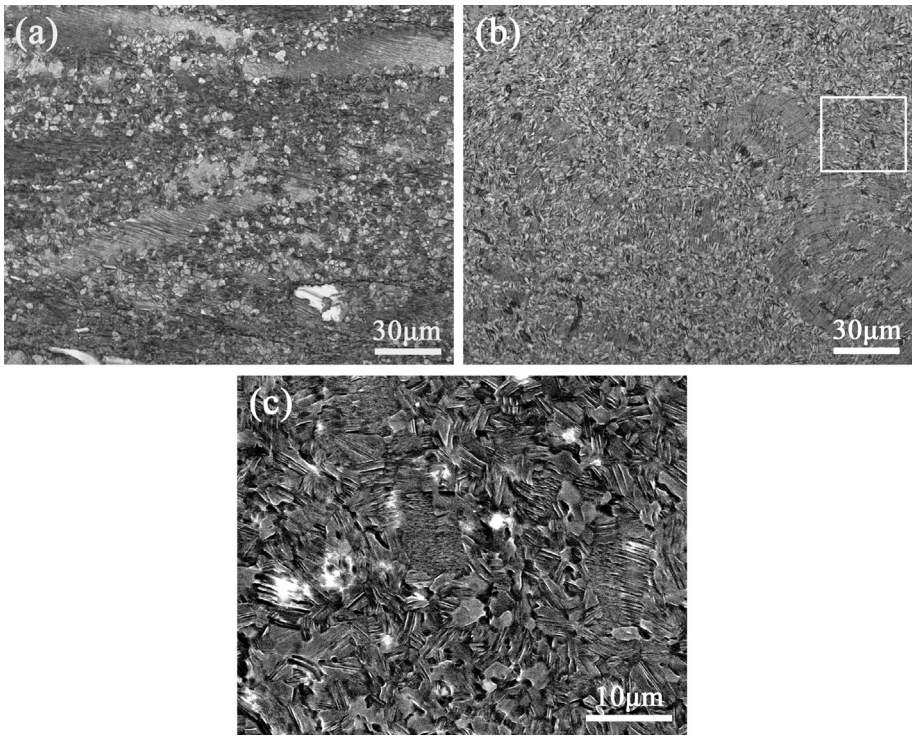

Fig. 2. Optical microstructures of extruded Mg-2Dy-0.5Zn alloy parallel to the extruded direction (a) and vertical to the extrusion direction (b), (c) is a high-magnification SEM image of white frame in image (b).

$\sigma_{0.2}$, σ_b and ε of Mg-2Dy-0.5Zn alloy are 245 MPa, 260 MPa and 36% at 300 °C, respectively, which are much higher than those of the as-cast $Mg_{97}Zn_1Y_2$ alloy (92 MPa, 135 MPa and 10% at 250 °C) [19]. The excellent tensile properties of extruded alloy are mainly ascribed to the grain refinement and precipitation strengthening of LPSO phase with high thermal stability. On the contrast, the large grain size and the coarse $Mg_{12}Zn_1Y_2$ phases with LPSO structure result in the lower tensile properties of as-cast $Mg_{97}Zn_1Y_2$ alloy, despite the alloy contains a great number of these phases. The large difference in mechanical properties of two alloys also affects the friction and wear properties.

3.2. Wear behavior

Fig. 4 displays the variation in coefficient of friction with load for extruded Mg-2Dy-0.5Zn alloy and as-cast $Mg_{97}Zn_1Y_2$ alloy. The coefficient of friction of two alloys sharply decreases at low load (0–100 N) and then gradually decreases at medium load (100–380 N) and finally reaches the lowest value at 380 N and 760 N for as-cast $Mg_{97}Zn_1Y_2$ alloy and extruded Mg-2Dy-0.5Zn alloy, respectively. It is noted that two alloys exhibit a similar trend in the coefficient of friction with increasing load, despite extruded Mg-2Dy-0.5Zn alloy displays a lower coefficient of friction as compared with as-

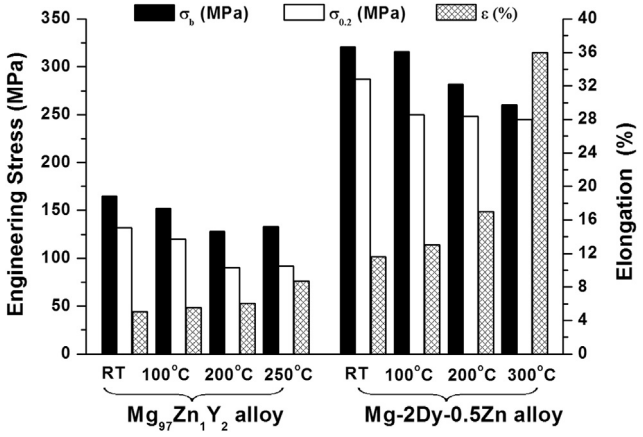

Fig. 3. Tensile properties of extruded Mg-2Dy-0.5Zn and as-cast $Mg_{97}Zn_1Y_2$ alloys at different temperatures.

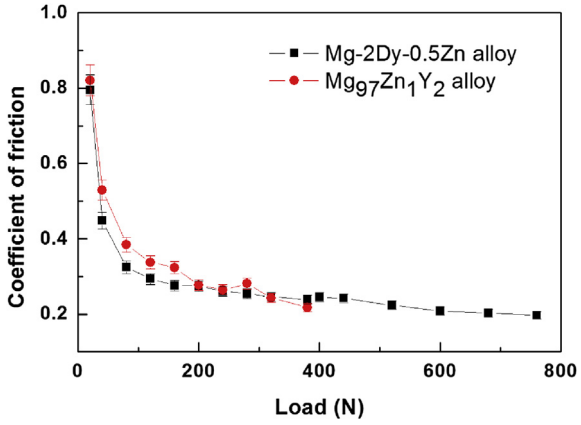

Fig. 4. Coefficients of friction of extruded Mg-2Dy-Zn and as-cast Mg97Zn1Y2 alloys at different applied loads.

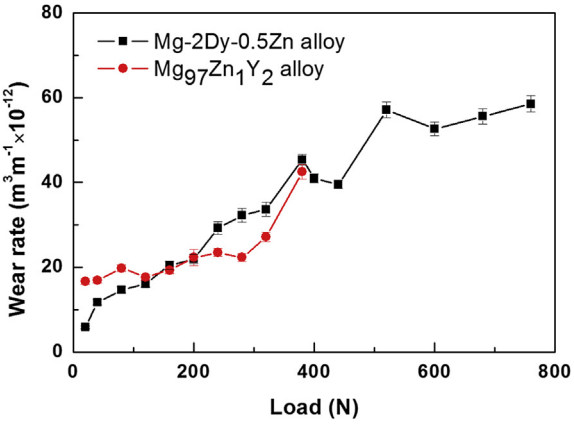

Fig. 5. Wear rates of extruded Mg-2Dy-Zn and as-cast $Mg_{97}Zn_1Y_2$ alloys at different applied loads.

cast $Mg_{97}Zn_1Y_2$ alloy at lower load (0–380 N). Fig. 5 shows the variation in wear rate with load for extruded Mg-2Dy-0.5Zn alloy and as-cast $Mg_{97}Zn_1Y_2$ alloy. The wear rate of as-cast $Mg_{97}Zn_1Y_2$ alloy gently increases until 280 N and then rapidly increases with increasing load, while that of extruded Mg-2Dy-0.5Zn alloy successively increases before 380 N and suddenly decreases at 450 N and then increases rapidly. It can be seen from Fig. 5 that there exists a large difference in variation region of wear rate with applied load for two alloys. This suggests that two alloys exhibit different wear mechanism at different load region. SEM images of the worn surface of extruded Mg-2Dy-0.5Zn alloy at different load are shown in Fig. 6. A great number of grooves with plastic deformation and cracks appear on the worn surface at lower load (20–200 N). The grooves mainly distribute along the sliding direction and the cracks form around the plastic deformation region. These are typical features of abrasion and delamination wear mechanisms, in which hard particles in between contracting surfaces, plough or cut into the pin, causing wear by removal of small fragments [24,25]. At a load of 380 N, some fine abrasive joints appear on the worn surface (Fig. 6(c)). This is a typical feature of adhesion. With increasing load, the grooves generally become wide and shallow as shown in Fig. 6. Simultaneously, as the load increases, the rise of surface temperature caused by frictional heating leads to the

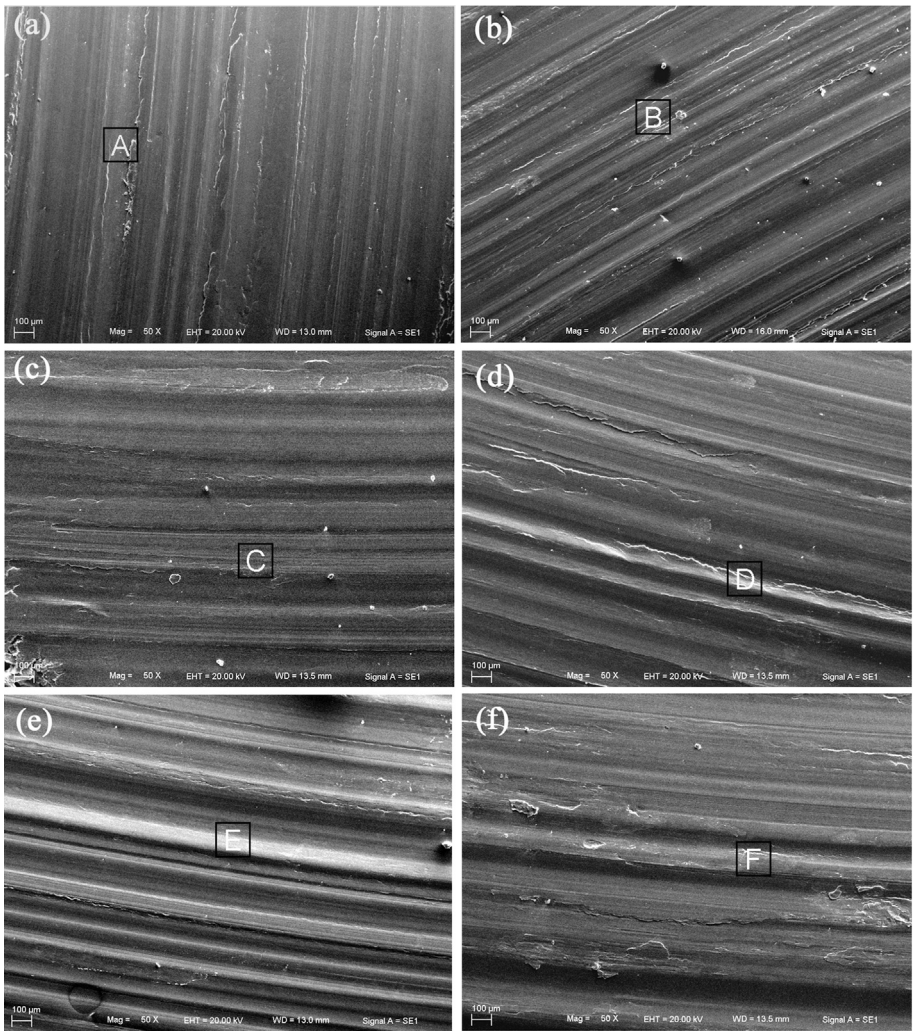

Fig. 6. SEM micrographs of worn surface of alloy at different applied loads: (a) 20 N, (b) 200 N, (c) 380 N, (d) 440 N, (e) 520 N and (f) 760 N.

Table 1
EDS analysis of worn surface for the alloy in Fig. 6.

Testing area	Mg (wt.%)	Dy (wt.%)	Zn (wt.%)	O (wt.%)	Totals
A	82	10.4	2.8	4.8	100
B	69.9	10.7	2.9	16.4	100
C	60.4	10.2	2.4	27	100
D	55.3	7.5	1.1	36.1	100
E	74.2	9.8	0.9	15.1	100
F	78.1	10.5	0.7	10.7	100

decrease of yield strength and the increase of ductility (see Fig. 3). The material is easy to generate plastic deformation and they spread out of the contact surface as well as by moving side away. The similar finding of material extrusion was reported in other Mg alloys and their composites [26–28]. At high loads of 520 N and 760 N, severe plastic deformation and plastic yielding occur on the worn surface (see Fig. 6(e) and (f)). This morphology is associated with thermal softening and melting of alloy caused by frictional heating at the sliding interface [29]. Nevertheless, it is worth noting that magnesium is easy to be oxidized to magnesium oxide during friction between pin and counter steel disc. Also, the EDS results in Table 1 indicate that the amount of atomic oxygen at the worn surface of alloy firstly increases and then decreases with increasing load. The similar results were reported in other magnesium alloys [30]. The amount of atomic oxygen reaches a highest value of 36.1% at 440 N and the others are Dy, Mg and Zn elements, respectively. At this moment, the thick oxide layer contained Dy and Zn element formed at the worn surface and could effectively protect the sliding surface and further increase friction coefficient and decrease wear rate [19]. As a result, the lower worn rate at 380–440 N in Fig. 5 indicates the oxide wear mainly dominates the wear behavior. Therefore, it can be seen that the formation of oxide layer is helpful to improving the wear resistant properties of alloy.

To clearly understand the wear mechanism of extruded Mg-2Dy-0.5Zn alloy, the morphologies of worn surface around the periphery at different load are shown in Fig. 7. In addition to the obvious abrasive and adhere wear marks, there is not exist extruded layer at the worn surface around the periphery as

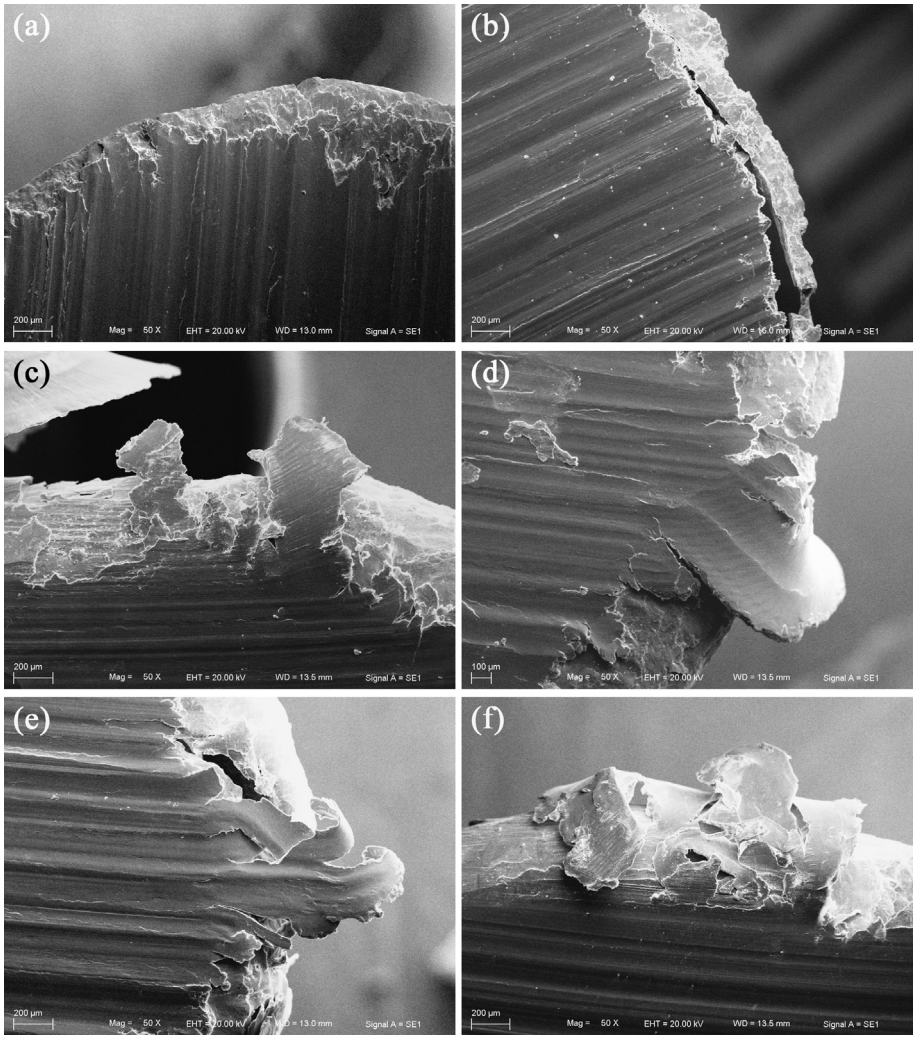

Fig. 7. SEM micrographs of worn surface of alloy around the periphery at different applied loads: (a) 20 N, (b) 200 N, (c) 380 N, (d) 440 N, (e) 520 N and (f) 760 N.

shown in Fig. 7 (a) and (b). With an increase of the load up to 380 and 440 N, the squamiform-shape edges of extruded layer and continuous oxide layer form, respectively, as shown in Fig. 7(c) and (d). When the load increases from 440 to 520 N, the oxide layer is delaminated at the worn surface, resulting higher wear rate (see Fig. 5). As the load is over 520 N, a combination of smooth surface and extruded layers at the worn surface as shown in Fig. 7(e) and (f), indicating surface melting is the main wear mechanism. However, for as-cast $Mg_{97}Zn_1Y_2$ alloy, the abrasion and delamination wear mechanisms occur at a load rang of 20–200 N, the thermal softening does at 240–280 N, and the surface melting become the dominate wear mechanism as load is over 280 N. So, it can be seen that extruded Mg-2Dy-0.5Zn alloy exhibit better wear resistance than as-cast $Mg_{97}Zn_1Y_2$ alloy under given conditions.

3.3. Contact surface temperature and its effect on wear behavior

When two contacting solids occur to slide, the heat appears at the surface of two solids resulted from the work is done against friction. As a result, the surface temperature increases with the proceeding of friction. The average surface temperature T_b (bulk temperature) can be measured by the expression [31]: $T_b = T_0 + \frac{\alpha\mu F v l_b}{A_n K_m}$, where T_0 is the temperature of the heat sink where the heat flows, α is the fraction of the heat diffusion into the pin, μ is the coefficient, F is the normal force on the pin, v is the sliding velocity, l_b is the mean diffusion distance, A_n is the normal contact area and K_m is the thermal conductivity. The variation in surface temperature with load for both extruded Mg-2Dy-0.5Zn alloy and as-cast $Mg_{97}Zn_1Y_2$ alloy is shown in Fig. 8. The thermal conductivity is 64 J/ms K for as-cast $Mg_{97}Zn_1Y_2$ alloy and 45 J/ms K for extruded Mg-2Dy-0.5Zn alloy. The surface temperature of two alloys increases with increasing load. It is noted that three temperature ranges appear in the curve, i.e., from room temperature to eutectic temperature, from eutectic temperature to liquidus temperature, above the liquidus temperature. This temperature range corresponds to 20–240 N for as-cast $Mg_{97}Zn_1Y_2$ alloy and 20–600 N for extruded Mg-2Dy-0.5Zn alloy, respectively. The thermal strength of the alloy plays an important role in wear properties in the range of room temperature and eutectic temperature. For as-cast $Mg_{97}Zn_1Y_2$ alloy, although the main strengthening $Mg_{12}ZnY$ phase distributed along the grain boundary could provide a good thermal stability below the eutectic temperature, the coarse grain size (30 μm) decreases the elevated temperature strengths. In contrast, for extruded Mg-2Dy-0.5Zn alloy, the dispersive distribution of LPSO phase in α-Mg grains and fine grain size (3 μm) significantly improve the tensile properties both at room and elevated temperature. The higher yield tensile strength and ultimate tensile strength of extruded Mg-2Dy-0.5Zn alloy than as-cast $Mg_{97}Zn_1Y_2$ alloy have been demonstrated in Fig. 3. According to the previous investigations [6,32], the fine grain size and good high-temperature properties could result in higher wear resistance properties. In addition, the ductility of extruded Mg-2Dy-0.5Zn alloy is obvious higher than that of as-cast $Mg_{97}Zn_1Y_2$ alloy both at room and elevated temperatures (see Fig. 3). Higher ductility could limit crack propagation and the delamination in the stress concentration sites and decrease wear rate of alloy [33]. Therefore, the extruded Mg-2Dy-0.5Zn alloy exhibits the better wear resistance than as-cast $Mg_{97}Zn_1Y_2$ alloy.

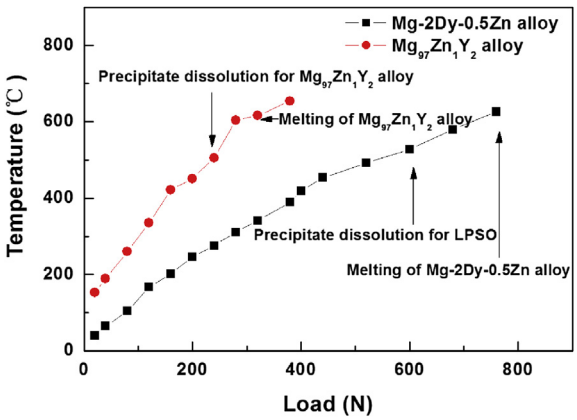

Fig. 8. The variation in surface temperature with applied load.

4. Conclusions

Pin-on-disk dry sliding tests of extruded Mg-2Dy-0.5Zn alloy (at.%) and as-cast $Mg_{97}Zn_1Y_2$ alloy against a steel conterface were carried out in load ranges of 20–760 N and 20–380 N, respectively. The wear rate and surface temperature of alloy increased with increase in applied load. The wear behavior of extruded Mg-2Dy-0.5Zn alloy can be classified into the mild region at 20–480 N and the severe region at 540–760 N. In mild region, abrasion, oxidation and delamination are main wear mechanisms. In contrast, in severe region thermal softening and melting were found to operate the wear behavior due to melting of LPSO phase and α-Mg matrix caused by higher surface temperature. The extruded Mg-2Dy-0.5Zn alloy exhibited the lower coefficient of friction and wear rate compared with as-cast $Mg_{97}Zn_1Y_2$ alloy. The improved wear resistance was mainly related to fine grain size, good thermal stability of LPSO phase and excellent higher-temperature mechanical properties.

Acknowledgments

This work was financially supported by the National Nature Science Foundations of China (No. 51301082, No. 51464031 and No. 51464032).

References

[1] H. Somekawa, A. Shimoda, T. Hirayama, T. Matsuoka, T. Mukai, Mater. Trans. 55 (2014) 216–219.
[2] A. Zafari, H. Ghasemi, R. Mahmudi, Wear 303 (2013) 98–108.

[3] Y. Liu, B. Jin, S. Shao, D. Li, X. Zeng, C. Xu, Tribol. Trans. 57 (2014) 275−282.
[4] Y. Liu, S. Shao, C. Xu, X. Yang, D. Lu, Mater. Lett. 76 (2012) 201−204.
[5] J. Xu, X. Wang, X. Zhu, M. Shirooyeh, J. Wongsa-Ngam, D. Shan, B. Guo, T.G. Langdon, J. Mater. Sci. 48 (2013) 4117−4127.
[6] S. Ramanathan, J. Alloys Compd. 502 (2010) 495−502.
[7] L. Falcon-Franco, E. Bedolla-Becerril, J. Lemus-Ruiz, J. Gonzalez-Rodríguez, R. Guardian, I. Rosales, Compos. Part B-Eng. 42 (2011) 275−279.
[8] E. Abe, Y. Kawamura, K. Hayashi, A. Inoue, Acta Mater. 50 (2002) 3845−3857.
[9] Y. Chino, M. Mabuchi, S. Hagiwara, H. Iwasaki, A. Yamamoto, H. Tsubakino, Scr. Mater. 51 (2004) 711−714.
[10] T. Itoi, T. Seimiya, Y. Kawamura, M. Hirohashi, Scr. Mater. 51 (2004) 107−111.
[11] Y. Kawamura, M. Yamasaki, Mater. Trans. 48 (2007) 2986−2992.
[12] Y. Zhu, A. Morton, J. Nie, Acta Mater. 58 (2010) 2936−2947.
[13] X. Shao, Z. Yang, X. Ma, Acta Mater. 58 (2010) 4760−4771.
[14] M. Yamasaki, T. Anan, S. Yoshimoto, Y. Kawamura, Scr. Mater. 53 (2005) 799−803.
[15] J. Wang, P. Song, S. Gao, X. Huang, Z. Shi, F. Pan, Mater. Sci. Eng. A 528 (2011) 5914−5920.
[16] G. Bi, D. Fang, L. Zhao, Q. Zhang, J. Lian, Q. Jiang, Z. Jiang, J. Alloys Compd. 509 (2011) 8268−8275.
[17] L. Zhang, J. Zhang, Z. Leng, S. Liu, Q. Yang, R. Wu, M. Zhang, Mater. Des. 54 (2014) 256−263.
[18] G. Bi, D. Fang, L. Zhao, J. Lian, Q. Jiang, Z. Jiang, Mater. Sci. Eng. A 528 (2011) 3609−3614.
[19] J. An, R. Li, Y. Lu, C. Chen, Y. Xu, X. Chen, L. Wang, Wear 265 (2008) 97−104.
[20] M. Hu, Q. Wang, C. Li, W. Ding, Trans. Nonferrous Met. Soc. China 22 (2012) 1918−1923.
[21] G. Bi, Y. Li, S. Zang, J. Zhang, Y. Ma, Y. Hao, J. Magn. Alloys 2 (2014) 64−71.
[22] M.M.B. Avedesian, H. Baker, ASM Specialty Handbook: Magnesium and Magnesium Alloys, ASM International, Materials Park, OH, 1999.
[23] Q. Peng, J. Guo, H. Fu, X. Cai, Y. Wang, B. Liu, Z. Xu, Sci. Rep. 4 (2014) 1−5.
[24] A.K. Mondal, S. Kumar, Wear 267 (2009) 458−466.
[25] M. Hu, Q. Wang, C. Chen, D. Yin, W. Ding, Z. Ji, Mater. Des. 42 (2012) 223−229.
[26] A.-W. El-Morsy, Mater. Sci. Eng. A 473 (2008) 330−335.
[27] H. Chen, A. Alpas, Wear 246 (2000) 106−116.
[28] S. Ramanathan, Mater. Des. 31 (2010) 1930−1936.
[29] A. Zafari, H.M. Ghasemi, R. Mahmudi, Wear 292−293 (2012) 33−40.
[30] C. Taltavull, B. Torres, A.J. López, J. Rams, Wear 301 (2013) 615−625.
[31] S. Lim, M. Ashby, J. Brunton, Acta Metall. 35 (1987) 1343−1348.
[32] M. Habibnejad-Korayem, R. Mahmudi, H.M. Ghasemi, W.J. Poole, Wear 268 (2010) 405−412.
[33] G.E. Dieter, Mechanical Metallurgy (SI Metric Edition), third ed., McGraw-Hill, London, 1986.